\$ SUPER

Contents lists available at ScienceDirect

Biophysical Chemistry

journal homepage: www.elsevier.com/locate/biophyschem





Osmotic stress studies of G-protein-coupled receptor rhodopsin activation

Andrey V. Struts ^{a,b}, Alexander V. Barmasov ^{c,d}, Steven D.E. Fried ^e, Kushani S.K. Hewage ^a, Suchithranga M.D.C. Perera ^a, Michael F. Brown ^{a,f,*}

- ^a Department of Chemistry and Biochemistry, University of Arizona, Tucson, AZ 85721, USA
- b Laboratory of Biomolecular NMR, St.-Petersburg State University, 199034 St.-Petersburg, Russia
- ^c Department of Biophysics, St.-Petersburg State Pediatric Medical University, 194100 St.-Petersburg, Russia
- ^d Department of Physics, St.-Petersburg State University, 199034 St.-Petersburg, Russia
- Department of Chemistry, Stanford University, Stanford, CA 94305, USA
- f Department of Physics, University of Arizona, Tucson, AZ 85721, USA

ARTICLE INFO

Keywords: G-protein-coupled receptors Membranes Optical spectroscopy Rhodopsin Signal transduction Vision

ABSTRACT

We summarize and critically review osmotic stress studies of the G-protein-coupled receptor rhodopsin. Although small amounts of structural water are present in these receptors, the effect of bulk water on their function remains uncertain. Studies of the influences of osmotic stress on the GPCR archetype rhodopsin have given insights into the functional role of water in receptor activation. Experimental work has discovered that osmolytes shift the metarhodopsin equilibrium after photoactivation, either to the active or inactive conformations according to their molar mass. At least 80 water molecules are found to enter rhodopsin in the transition to the photoreceptor active state. We infer that this movement of water is both necessary and sufficient for receptor activation. If the water influx is prevented, e.g., by large polymer osmolytes or by dehydration, then the receptor functional transition is back shifted. These findings imply a new paradigm in which rhodopsin becomes solvent swollen in the activation mechanism. Water thus acts as an allosteric modulator of function for rhodopsin-like receptors in lipid membranes.

1. Introduction

G-protein-coupled receptors (GPCRs) are membrane-spanning proteins implicated in the regulation of various biological processes in eukaryotes by transmitting signals across cellular membranes. Somewhere around 30 to 50% of drugs target diseases linked to dysfunctions of pathways of rhodopsin-like receptors [1-4]. In recent years dozens of GPCR structures have become available based on advances in their crystallization [5–7]. Despite the great amount of structural information provided by X-ray analysis, however, the experimental conditions involved in crystallization render these studies strikingly incomplete. The use of cryogenic temperatures, dehydration, and absence of a lipid membrane reduce the dynamic allostery of the various receptor states to a single representative structure. On the other hand, recent investigations of rhodopsin by small-angle and quasielastic neutron scattering reveal that solvent swelling of the receptor occurs by water absorption upon activation [8,9], a conclusion that is also supported by all-atom molecular dynamics (MD) simulations [10,11]. In contrast to ion channels and aquaporins, the role of water in GPCR mechanisms is only now becoming understood. Wide-angle X-ray scattering (WAXS) studies [12] further indicate that at ambient temperature the structural changes of rhodopsin due to light activation may be greater than those revealed previously by X-ray crystallography. Additional quantitative data are thus needed on the changes in rhodopsin volume in the active state.

As an example, Fig. 1 illustrates the first steps of the signal transduction process of rhodopsin. Conversion of the ligand retinal by light absorption (Fig. 1a) into an agonist leads to the receptor activating conformational changes (Fig. 1b). The activated receptor then binds the heterotrimeric G-protein (Fig. 1c), which triggers exchange of GTP for GDP on the G-protein α -subunit, followed by its dissociation and interaction of the subunits with other intracellular proteins in the signal transduction cascade. Further understanding of rhodopsin-based signaling requires that the effects of water and the membrane lipids on the receptor should be considered (the so-called soft matter) [13,14]. Here we review our novel experimental strategy that yields transformative new insights into the role of bulk water in rhodopsin activation. To observe the large-scale hydration-coupling interactions that are

^{*} Corresponding author at: Department of Chemistry and Biochemistry, University of Arizona, Tucson, AZ 85721, USA. *E-mail address:* mfbrown@arizona.edu (M.F. Brown).

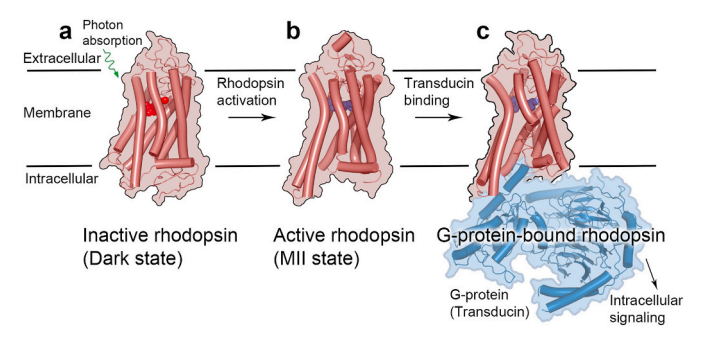


Fig. 1. Signal transmission by G-protein-coupled receptor rhodopsin entails conformational changes and dynamic allostery. (a) Ligand transformation into agonist upon photonic absorption leads to (b) rhodopsin activating conformational changes. (c) Active receptor forms heterotrimeric complex with G-protein. Exchange of GDP with GTP leads to dissociation of G_{α} subunit from the $G_{\beta\gamma}$ subunits and the receptor. Interaction of the subunits with intracellular effector proteins continues the signal transduction cascade. Understanding GPCR signaling also involves effects of the lipid membrane environment.

typically invisible to structural methods like X-ray crystallography or cryogenic electron microscopy, we describe a unique approach that shows how an influx of bulk water stabilizes the active rhodopsin conformation. In addition, we discuss the role of the aqueous solvent in activation—which surprisingly turns out to be much more significant than simply giving a medium for organizing the cellular components.

2. Hydration changes of rhodopsin are observed upon light activation

Rhodopsin activation occurs upon absorption of a photon of visible light by 11-cis retinal, followed by its isomerization to the all-trans conformation. The reaction mechanism for rhodopsin can be summarized by the time-ordered activation sequence [15–18]: Rh + $h\nu \rightarrow MI \rightleftharpoons$ $MII_a \rightleftharpoons MII_b + H_3O^+ \rightleftharpoons MII_bH^+$, where Rh is dark-state rhodopsin with its 11-cis retinal covalently bound by a protonated Schiff base linkage, MI represents the preactive state with all-trans retinal and a protonated Schiff base, MIIa is the state with a deprotonated Schiff base but in the inactive conformation, MII_b indicates the active state, and MII_bH⁺ is the active state further stabilized with Glu¹³⁴ of the E(D)RY motif protonated. Notably, the last four states populate a high-dimensional energy landscape and are in dynamic equilibrium after photoactivation, which can be biased according to the thermodynamic state variables (pH, temperature, or membrane composition) [14,17,19,20]. The MII_b states entails rotation of the cytoplasmic end of transmembrane helix 6 (TM6) away from the rest of the helical bundle, thereby opening the binding pocket for the transducin G-protein (Gt). In terms of structural biology, the activating movement of the helix TM6 together with elongation of helix TM5 are suggestive of greater receptor volume and internal hydration [5,9,18,21,22].

Previous applications of osmotic stress methodology [23,24] have determined changes in the number of water molecules associated with the activity of soluble proteins such as hemoglobin [23], hexokinase [24], and adenosine deaminase [25]. In addition, membrane proteins and peptides have been investigated, including potassium channels [26], alamecithin [27], sodium channels [28], and cytochrome *c* oxidase [29]. For membrane proteins, it is required to consider the interactions of water with the membrane lipid bilayer [30–32]. Changes in water activity affect phospholipid acyl chain packing [33], the bilayer thickness and interfacial area per lipid molecule [30,34], membrane curvature [14], and the phospholipid lateral diffusion coefficients [35]. Earlier studies of visual rhodopsin have investigated the effect of hydration on its activation and on acyl chain packing in the retinal disk membranes (RDM) using small osmolytes such as glycerol, sucrose, and

stachyose [36]. An example of deconvoluted difference spectra for the MI–MII rhodopsin equilibrium in the RDM is shown in Fig. 2a. Data are included for rhodopsin measured for the dark state, after partial bleaching, following addition of hydroxylamine, and after complete bleaching in the presence of hydroxylamine. The equilibrium constant for the transition from the preactive MI to the active MII state, K = [MII]/[MI], was established from the electronic (UV/visible) absorption bands of MI and MII (Fig. 2a) [37]. Fig. 2b demonstrates the effects of small osmolytes on the MI–MII equilibrium constant, K, at T = 20 and 35 °C. Notably, these studies have concluded that an *efflux* of water occurs from the photoreceptor upon light activation.

In terms of equilibrium thermodynamics, the change in the number of water molecules associated with the protein upon activation, $\Delta N_{\rm w}$, can be determined from the slope of the $\ln K$ value versus the osmolyte concentration [38]:

$$\ln K = -\Delta N_{\rm w} \frac{[\text{osmolal}]}{55.6}.\tag{1}$$

In the above formula, the ln K dependence for small osmolytes indicates the solution osmolality increases the equilibrium concentration of the MII state. The shift of the metarhodopsin equilibrium to the active MII state by osmolytes thus implies that this state is less hydrated, by Le Châtelier's principle. In this way, it has been estimated that 20 water molecules are released during the MI-to-MII transition at 20 °C, and that 13 waters are released at 35 °C [36]. Moreover, biophysical analysis of the fluorescence anisotropy decay of 1,6-diphenyl-1,3,5-hexatriene (DPH) in terms of the rotational diffusion model has revealed that the angular distribution of DPH about the membrane normal was narrowed with greater osmolality [36], suggestive of an increase of the acyl chain packing in membranes. Lower hydration of MII agrees with X-ray crystallographic studies, which are insensitive to the bulk water movement upon receptor activation and reveal only a few structural water molecules present in the dark and the active states of rhodopsin. Yet these findings present an enigma—e.g., they disagree with previous molecular dynamics (MD) studies [10,39,40] suggesting that an influx of water occurs upon light activation (Fig. 3). They are also inconsistent with the reactivity of retinal to hydrolysis by hydroxylamine (Fig. 2a) at the MII stage of the photolytic pathway [41]. Lastly, our neutron scattering studies furthermore indicate that rhodopsin hydration and the radius of gyration both increase in the activation process [8,9]. Hence the prior

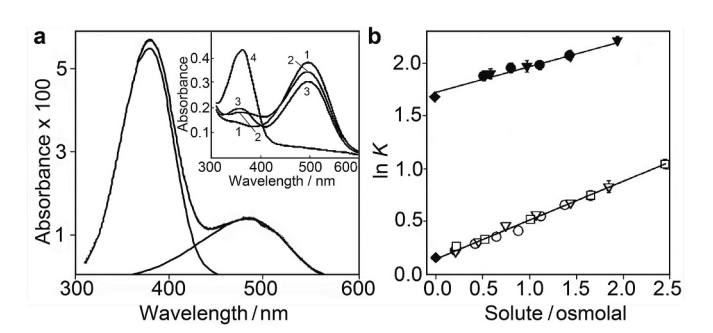


Fig. 2. Formation of light-activated state of visual rhodopsin depends on membrane hydration. (a) Example of deconvoluted difference spectra for MI–MII rhodopsin equilibrium in retinal disk membranes at pH 7.0 and T=30 °C with individual (right) MI and (left) MII spectra. Inset: absorption spectra of rhodopsin. Spectra were measured (1) before bleaching, (2) after partial bleaching, (3) following addition of hydroxylamine, and (4) after complete bleaching in the presence of hydroxylamine. (b) Effects of solute osmolality on equilibrium constant K for the MI–MII equilibrium at T=20 and 35 °C. The slope of each line equals $-\Delta N_{\rm w}/55.6$, where $\Delta N_{\rm w}$ is the change in the number of water molecules in solute-inaccessible protein regions. (c) Glycerol, 20 °C; (∇) sucrose, 20 °C; (\square) stachyose, 20 °C; (\square) glycerol, 35 °C; and (\square) sucrose, 35 °C; (\square) control, both temperatures. Adapted from refs. [36, 37]. Copyright 1999 American Chemical Society.

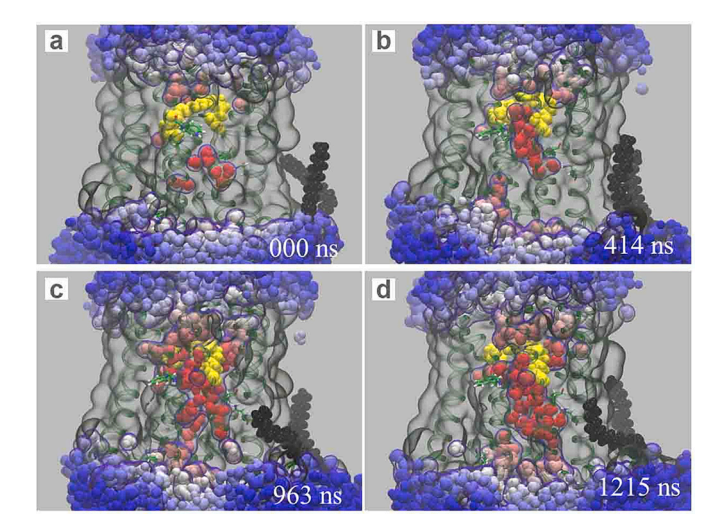


Fig. 3. Molecular dynamics simulations of rhodopsin reveal influx of bulk water upon light activation. Snapshots of all-atom molecular dynamics (MD) simulation of rhodopsin at (a) 0 ns, (b) 414 ns, (c) 963 ns, and (d) 1215 ns after retinal isomerization in silico [10]. Internal water molecules (red) flood the transducin binding cleft forming a channel to the retinal ligand.

results raise the question: Is the active MII state more or less hydrated versus the inactive dark state?

To resolve this puzzle, we studied the influence of hydration on rhodopsin activation using a series of hydrophilic polymer osmolytes with different molar masses [42] (Fig. 4). Water-soluble polymers (polyethylene glycol, PEG) were introduced for rhodopsin hydration control due to the relatively large osmotic pressures (Π) that can be attained (>10 MPa). The fraction of the active MII state was established by UV/visible electronic spectroscopy (Fig. 4a). Difference spectra of rhodopsin (light minus dark states) in retinal disk membranes (Fig. 4a) were fit by a linear combination of the basis difference spectra of the MI, $\Delta A_{\rm MI}(\lambda)$, and MII, $\Delta A_{\rm MII}(\lambda)$, states determined experimentally at pH 9.5 and 10 °C or pH 5 and 21 °C respectively: $\Delta A(\lambda) = c_1 \Delta A_{MI}(\lambda) +$ $c_2\Delta A_{\rm MII}(\lambda)$ [43]. The fraction of the active MII state, θ , was determined by the relative contribution of its basis spectrum, $\theta = c_2/(c_1 + c_2)$ (Fig. 4a). Notably, the pH titration curves (Fig. 4a) establish how the polymer osmolytes reversibly shift the metarhodopsin equilibrium to either the preactive (closed) MI state or the active (open) MII state. By the law of mass action, for a protein like rhodopsin, the back shifting of the equilibrium to the preactive MI state means that in the forward direction (transition from MI to MII state) an influx (flood) of water occurs. The isotherms for different osmolytes (ln K versus Π) (Fig. 4b) reveal a negative slope for large relative molar mass (M_r) osmolytes (PEG 1500 and PEG 400), while a positive slope is seen for small osmolytes (PEG 300 and PEG 200). Consequently, osmolytes with a large molar mass favor the inactive MI state (closed conformation). On the other hand, small osmolytes increase the active (open) MII fraction in agreement with previous work [36]. Because of the withdrawal of water observed by large osmolytes and the shift of the equilibrium to the inactive MI state, we conclude at this point that the active MII state is actually more hvdrated.

Accordingly, we thus suggest that previous conclusions [36] are based on usage of relatively small osmolytes, which penetrate the transducin (G-protein) binding cavity and cannot withdraw water from the receptor at relatively low concentrations (see below). For reasons of penetration, the number of water molecules that enter rhodopsin upon light activation should be calculated for the largest osmolytes, which are most excluded from the protein. Clearly, the conjugate variables are the hydrated volume $(V_{\rm w})$ and the osmotic pressure (Π). The equilibrium constant (K= [MII]/[MI]) thus depends on osmotic pressure Π and reads:

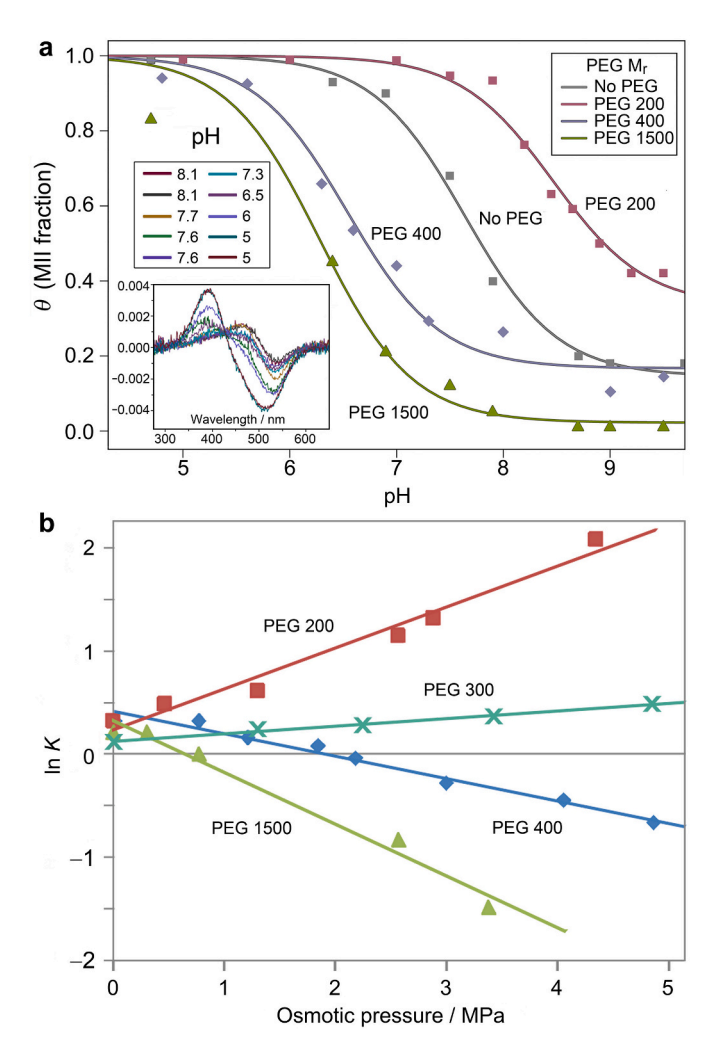


Fig. 4. Osmotic stress experiments reveal shifting of metarhodopsin equilibrium depends on polymer osmolyte size. (a) Fraction of active MII state (θ) versus pH showing effect of controlled hydration ($T=15\,^{\circ}$ C) for osmolytes of different molar mass (M_r) (30–35% w/w polyethylene glycol, PEG). Inset: representative electronic UV/visible difference absorption spectra of rhodopsin (photobleached minus dark state). (b) Metarhodopsin (MII/MI) ratio ($\ln K$) plotted versus osmotic pressure (Π) for different size PEG osmolytes (pH 7.4, $T=15\,^{\circ}$ C). Forward or back shifting of the metarhodopsin equilibrium occurs for small or large polymer (PEG) osmolytes, respectively. Adapted from ref. [42]. Reproduced by permission of Wiley-VCH Verlag GmbH & Co. KGaA, Weinheim.

$$\left(\frac{\partial \ln K}{\partial \Pi}\right)_T = -\frac{\Delta V^{\circ}}{RT}.\tag{2}$$

Here $\Delta V^{\circ} \approx N_{\rm w} \bar{V}_{\rm w}$ is the standard change in excess (partial) water volume of the initial and final states, $N_{\rm w}$ is the number of water molecules, and $\bar{V}_{\rm w}$ is the partial molar water volume. By this method, we estimate approximately 80 water molecules as a lower limit to the influx of water upon light activation (Fig. 5). For partially excluded polymers (< PEG 400), the apparent volume change is given by $\Delta V_{\rm app} = \Delta V^{\circ}(1-P)$, where P is the partition coefficient between the protein and the solution. It follows that there can be a reduction of the apparent hydrated volume of rhodopsin upon activation in the presence of the small osmolytes, but the $\Delta V_{\rm app}$ values should remain positive. Still, in our experiments we observe a reversal of sign of the $\Delta V_{\rm app}$ values for small osmolytes (PEG 200, PEG 300). Evidently, the negative apparent hydrated volume is not related to withdrawal of water by small osmolytes, but rather to shifting of the metarhodopsin equilibrium to the active MII state due to

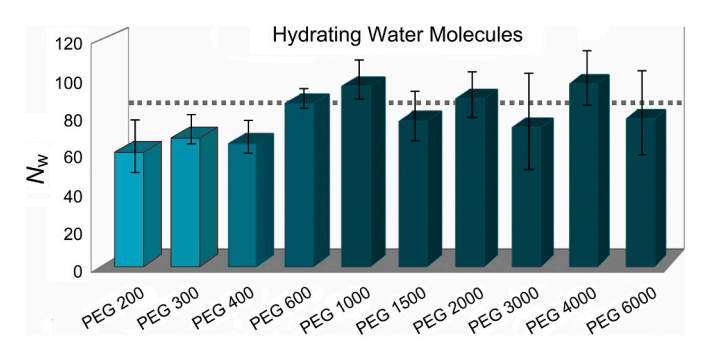


Fig. 5. Light activation of rhodopsin leads to a large influx of water molecules into the protein. Osmotic stress data for hydrophilic polymers reveal numbers of water molecules ($N_{\rm w}$) entering rhodopsin as indicated for various-sized polyethylene glycols (PEGs). Smaller PEGs show smaller apparent water influx than more excluded large PEGs. The number of water molecules determined by the universal large osmolyte response(\sim 80–100) is indicated by the dotted line. Adapted from ref. [43]. Copyright (2022) National Academy of Sciences.

additional interactions.

One possible interpretation is that this trend is due to the interaction of small osmolytes with lipids, because the osmolyte interaction with the protein is smaller due to partial or complete penetration into the transducin binding cavity. In that case, membrane dehydration could increase the bilayer thickness as strikingly demonstrated by solid-state 2 H NMR spectroscopy [30,34] (Fig. 6). Examples of solid-state 2 H NMR spectra of DMPC lipids (Fig. 6a) show that for large osmolytes the quadrupolar splittings, $\Delta \nu_Q^{(i)}$, characterizing the carbon-deuterium bond order parameters increase with greater osmotic or hydrostatic pressure, indicating greater bilayer thickness and a smaller area per lipid (Fig. 6b, c). Increased thickness of the membrane bilayer generally supports rhodopsin activation. The volumetric chain thickness of the hydrocarbon layer, D_C , is related to the mean area per lipid, $\langle A \rangle$, according to

$$D_{\rm C} = \frac{2V_{\rm C}}{\langle A \rangle},\tag{3}$$

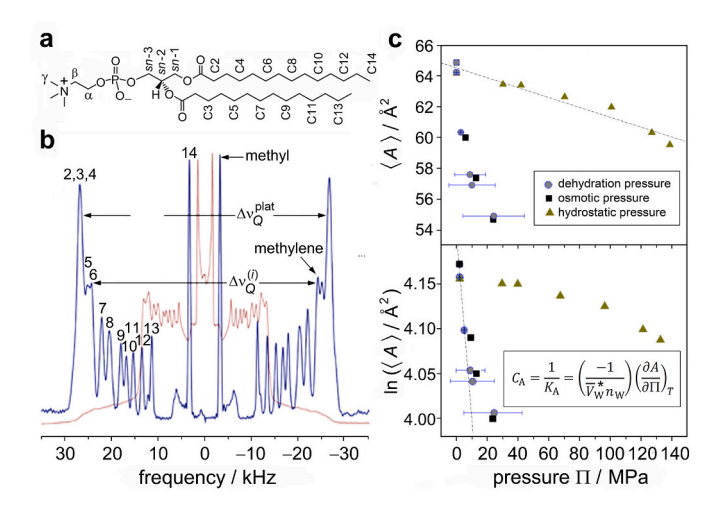


Fig. 6. Lipid membranes deform under osmotic or hydrostatic pressure as revealed by deuterium NMR spectroscopy. (a) Chemical structure of DMPC lipid molecule. (b) Solid-state $^2\mathrm{H}$ NMR spectra provide residual quadrupolar couplings (RQCs) and $C^{-2}\mathrm{H}$ bond order parameters for calculation of the membrane structure. (c) Mean-torque model gives area per lipid in the liquid-disordered (ld) state. Osmotic pressure of polymer solution leads to changes in area per lipid and elastic properties (area compressibility modulus 142 ± 30 mJ m $^{-2}$) that show emergence of elasticity from atomistic interactions. Force–based measurements thus reveal that osmotic and hydrostatic pressure affect lipid bilayer properties. Adapted from ref. [32]. Copyright (2011) Elsevier.

where $V_{\rm C}$ is the total volume of an individual acyl chain, which is given by the densitometry measurements of John Nagle and coworkers [44,45]. Dehydration can also lead to greater magnitude of the negative monolayer spontaneous curvature, as described by the flexible surface model (FSM) [14]. Both effects will facilitate active MII formation in lipid bilayers [14,41,46] in agreement with experimental observations for small osmolytes (Figs. 4b), but opposite to large osmolytes. Moreover, experimental site-directed spin labeling (SDSL) studies [47] of rhodopsin in n-Dodecyl- β -D-maltoside (DDM) micelles by Wayne Hubbell and coworkers have shown that the small osmolyte sucrose back shifts the population toward the preactive MI component. Because the forward shifting to MII is absent in the detergent-solubilized system, a role of the lipid bilayer is supported in favoring the active state in the presence of small osmolytes.

Additionally, the partial penetration of small osmolytes into the protein might withdraw water from smaller internal cavities associated with the MI–MII transition [4,5,48,49]. One example is afforded by recent hydration studies monitoring bound water by infrared spectroscopy in opsin and the E134Q mutant. The results suggest that Glu¹³⁴ of the conserved E(D)RY motif is a hydration site at the protein-lipid interface, which dehydrates going from MII_b to the MII_bH⁺ state [50]. Local dehydration of small protein regions such as these is in agreement with MII stabilization by small osmolytes [36] (see Fig. 4a, b). The shift to the active MII state could also be explicable by specific interaction of small osmolytes with the transducin binding cleft. Specific PEG-protein interactions are known to be inversely related to PEG size [51], although we did not observe any substantial binding of small osmolytes to rhodopsin (see below).

3. Hydration of photoactivated rhodopsin affects binding of G-protein-derived peptides

In general, peptide chemistry can contribute further important insights into molecular interactions of proteolipid membranes, as shown by the seminal work of Richard Epand and coworkers [52-55]. For rhodopsin in lipid membranes, we established that upon light activation greater hydration causes binding of C-terminal peptide derivatives of the α -helix of the cognate G-protein transducin, while dehydration drives unbinding [42]. Fig. 7 shows how the active MII fraction in the native RDM depends on concentration of the transducin C-terminal peptide analogue (amino acid sequence ILENLKDVGLF) when various osmolytes are present. Such peptides have a high binding affinity to rhodopsin and stabilize the active MII state when bound to the receptor [5,56-58]. Fitting the binding isotherms (Fig. 7 a, b) reveals that the larger polymers (PEG 1500 and PEG 400) decrease the binding affinity by an order of magnitude. This finding implies that the interaction of large osmolytes and the transducin peptide with the protein is competitive. On the other hand, for smaller osmolytes ($M_r < 400$ Da), the effect is absent (inset of Fig. 7a). As a result, small osmolytes do not compete for binding to rhodopsin with the transducin peptide, either because they do not bind to the protein or have much lower binding affinity. Further analysis indicates that for large osmolytes, the peptide binding constant correlates with proton uptake by Glu¹³⁴ of the conserved E(D)RY sequence motif. Hence, water not only affects the equilibrium between active and inactive states [59] of the receptor, but also governs the intrinsic binding of its cognate G-protein.

4. Extended osmolyte studies reveal effects on pH-dependent rhodopsin activation

Next, we conducted additional osmotic stress studies for a large range of pH values, osmolyte concentrations, and molar masses [43]. Fig. 8 shows that the effect of pH on rhodopsin activation in the pH range from 3 to 10 can be explained by an extended Henderson-Hasselbalch equation involving two pK_A values and a nonzero alkaline

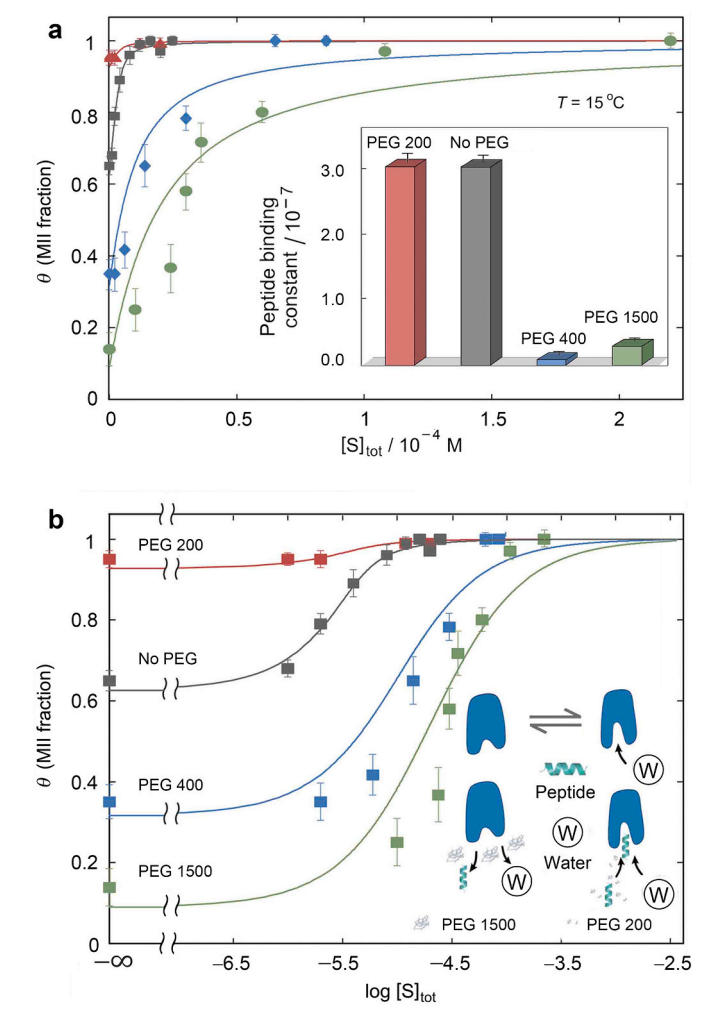


Fig. 7. Transducin C-terminal-derived peptide binding to light-activated rhodopsin depends on hydration. (a) Active MII fraction (θ) in native retinal disk membranes (RDM) versus total concentration ([S]_{tot}) of high-affinity transducin C-terminal peptide analogue (pH 7.4, $T=15\,^{\circ}$ C). Data are fit to a single-site binding isotherm. Inset: effect on peptide binding constant for different size polymer osmolytes. (b) Active MII fraction (θ) versus log [S]_{tot} value. Inset: Illustration of how C-terminal peptide competes with large osmolytes (PEG 1500) yet is noncompetitive for small osmolytes (PEG 200). Binding and unbinding of transducin-derived peptides occur due to hydration and dehydration of rhodopsin. Adapted from ref. [42]. Reproduced by permission of Wiley-VCH Verlag GmbH & Co. KGaA, Weinheim.

endpoint [15,17,41]. The main influence of PEG is its shifting of the apparent p K_A of Glu¹³⁴ following deprotonation of the Schiff base and breakage of the ionic lock with Glu¹¹³ [5,17]. Protonation of Glu¹³⁴ within the conserved E(D)RY motif is coupled to breaking another ionic lock involving Arg^{135} and Glu^{247} , and stabilizes the outward-tilted TM6 helical conformation of the active substate referred to as MII_b , or MII_bH^+ in the protonated case [17]. Hence, the pK_A of Glu^{134} characterizes the pH-dependent equilibrium between MI with a protonated Schiff base and the MII_bH⁺ substate with a deprotonated Schiff base (so-called anomalous pH dependence). Selectively stabilizing either the closed MI or open MII states by PEG affects this pK_A in addition to the protein environment around the Schiff base (e.g., hydration within the protein). Besides the pK_A describing the rhodopsin activation, the pH titration of rhodopsin also has a nonzero alkaline endpoint at greater temperatures, due to thermally activated MIIa and deprotonated MIIb substates (Fig. 8a) [17]. Both $\mathrm{MII}_{\mathrm{a}}$ and $\mathrm{MII}_{\mathrm{b}}$ have a deprotonated Schiff base with a maximum absorption at 380 nm, giving a nonzero apparent MII fraction

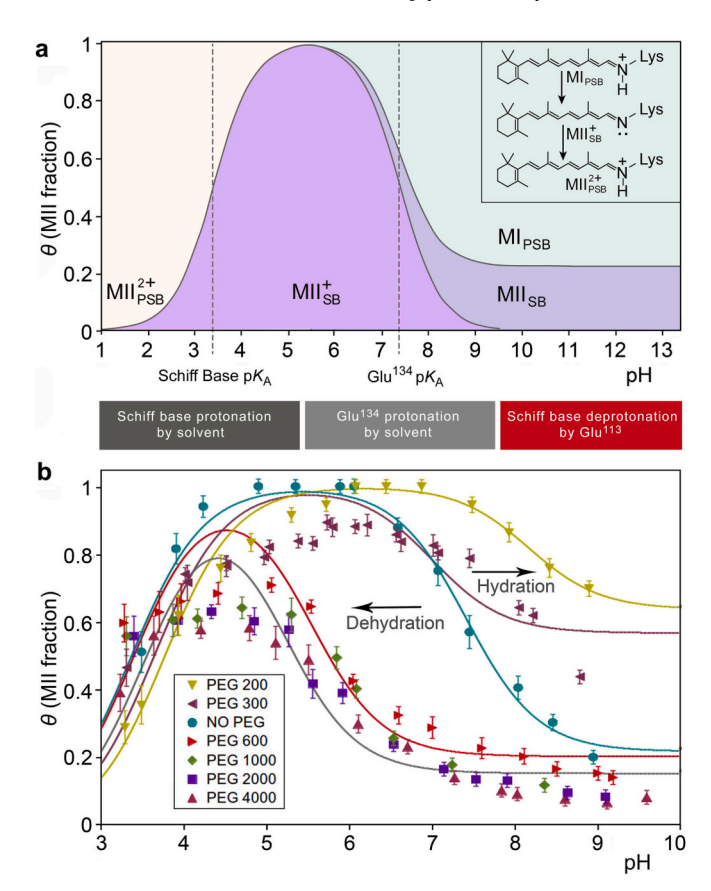


Fig. 8. Hydration reversibly shifts pH-dependent activation equilibrium of rhodopsin. (a) Influences of pH on rhodopsin activation involving highly conserved E(D)RY motif. The lower pK_A indicates protonation of the retinal Schiff base. The higher pK_A value (Glu¹³⁴ pK_A) indicates protonation of Glu¹³⁴ which stabilizes the fully active MII state. (b) Osmotic stress from large osmolytes (50% w/w at $T=15\,^{\circ}$ C) back shifts the apparent Glu¹³⁴ pK_A value from 7.4 to 5.2. At a saturating concentration of 30% w/w PEG 200 ($T=15\,^{\circ}$ C) the Glu¹³⁴ pK_A is maximally forward shifted to 8.2 favoring the active MII state. An osmolyte effect is also seen on the alkaline endpoint: small osmolytes stabilize the open MII_b conformation even when Glu¹³⁴ is fully deprotonated, increasing the alkaline endpoint, while dehydrating large osmolytes reduce the alkaline endpoint and hence the deprotonated MII_b population. Adapted from ref. [43]. Copyright (2022) National Academy of Sciences.

even at high pH values where little $\mathrm{MII_bH^+}$ is present [17]. Still, another factor to keep in mind is an additional p K_A under acidic conditions that manifests the protonation of the Schiff base in the $\mathrm{MII_bH^+}$ state [41]. As the retinylidene Schiff base protonates below this p K_A , the apparent MII fraction as established by UV–visible spectroscopy decreases (Fig. 8a).

It follows that the empirical pH-titration curve includes two p K_A values and an alkaline endpoint. The data may therefore be modeled by an extended Henderson-Hasselbalch formula for the active MII fraction θ that reads:

$$\theta(\text{pH}) = \frac{\theta_{\text{alk}} + 10^{\text{pK}_{A,\text{Glu}} - \text{pH}}}{1 + \left(1 + 10^{\text{pK}_{A,\text{SB}} - \text{pH}}\right)10^{\text{pK}_{A,\text{Glu}} - \text{pH}}}.$$
(4)

Here, $\theta_{\rm alk}$ denotes the alkaline endpoint (apparent MII fraction at high pH), while p $K_{\rm A,SB}$ characterizes the MII $_{\rm b}$ H $^+$ Schiff base protonation equilibrium and p $K_{\rm A,Glu}$ the Glu 134 protonation step (Fig. 8a). The pH titration data for the apparent MII fraction of rhodopsin in four different large- $M_{\rm r}$ PEG solutions were used to determine the model parameters. These results showed a striking p $K_{\rm A,Glu}$ shift from 7.4 to 5.1 in the presence of 50% (w/w) large polymer osmolytes (Fig. 8b). The pH titration curves for rhodopsin activation are analogous to pharmacological dose-response curves [17,42] where the ligand binding affinity is

changed by 2–3 orders of magnitude. This observed $pK_{A,Glu}$ shift implies a model in which large osmolytes dehydrate the receptor to shift its equilibrium to the closed MI state, stabilizing the intact ionic lock and giving a lower MII fraction. An apparent MII fraction of unity is typically not seen for these conditions, because of the MII_bH⁺ Schiff base protonation region of the titration curve, which begins to overlap with the predominant MI-MII_bH⁺ region. Remarkably, the large-M_r PEGs of different molar mass have identical behavior with a nearly equal $pK_{A Glu}$ shift, thus reinforcing the proposed universal osmotic effect by large polymers (Fig. 8b). In the range of the alkaline endpoint of the titration, base-catalyzed retinal hydrolysis follows photoactivation, yielding the apoprotein opsin. A quantifiable influence of PEG on the alkaline endpoint was extrapolated that was lowered by large polymer osmolytes. The results show that large PEGs destabilize the more open MII_b substate under high-pH conditions, where Glu¹³⁴ is fully deprotonated, agreeing with the pK_A shift that favors the closed MI state under osmotic pressure. In the case of small PEGs, the opposite effect is found, with forward shifting of the metarhodopsin equilibrium by intermediate concentrations of the osmolyte (Fig. 8b). For example, at a saturating concentration of 30% (w/w) of PEG 200, the titration curve has a p $K_{A,Glu}$ shift from 7.4 to 8.2 in the opposite direction to that seen for large PEGs. In total, there is a $pK_{A,Glu}$ difference of 3.1 units between the large and small PEG titration curves, showing the dramatic influence that osmolyte size poses for receptor hydration and proton transfer [60], together with activation. This magnitude of the pK_A shift is analogous to those observed for constitutive mutations of rhodopsin or retinoid antagonists

5. Compressibility of hydrated volume and osmolyte saturation of penetration are observed

It is also notable that the greater range of osmolyte concentrations and molar masses reveals apparent compressibility changes for large osmolytes, whereas saturation effects are observed for small osmolytes. Fig. 9 indicates that the dependence of ln *K* and correspondingly the

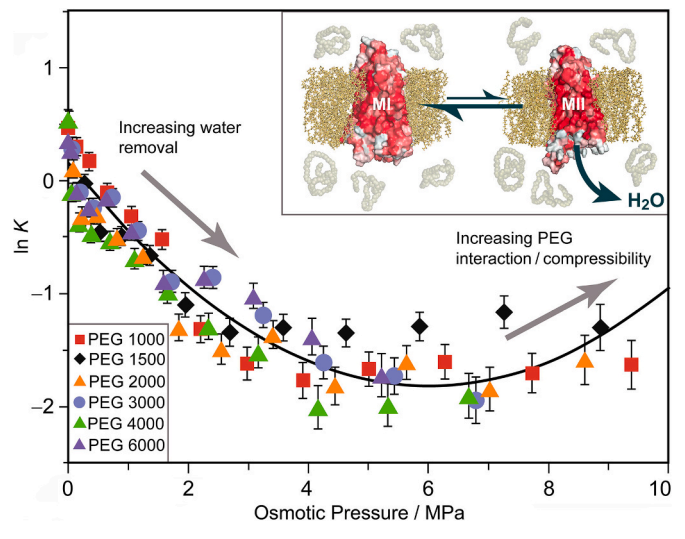


Fig. 9. Rhodopsin is dehydrated by large polymer osmolytes due to nonspecific colligative properties giving a universal osmotic response. Dehydration of visual rhodopsin by polyethylene glycol osmolytes is shown by natural logarithm of the MI–MII equilibrium constant (K = [MII]/[MI]) versus osmotic pressure of large PEGs which has an approximately second-order relationship. A universal colligative trend arises for PEGs of M_r between 1000 and 6000 Da with the linear term proportional to the change in hydrated volume. Inset: metarhodopsin equilibrium is shifted to the MI (closed) state by large polymer osmolytes which are entropically excluded and dehydrate the protein. Adapted from ref. [43]. Copyright (2022) National Academy of Sciences.

molar hydration volume on osmotic pressure is nonlinear. Hence, the second-order term needs to be considered in the virial expansion of $\ln K$ as a function of osmotic pressure, which is given by:

$$\ln K = \ln K^{\circ} - \left(\frac{\Delta V^{\circ}}{RT}\right) \Pi + \left(\frac{1}{2}\Delta C\right) \Pi^{2}. \tag{5}$$

Fitting the experimental data with this quadratic function gives the change in protein hydrating volume ΔV° between MI and MII and the number of hydrating water molecules per mole of rhodopsin $N_{\rm w}$ under standard-state (zero osmotic pressure) conditions. Introducing the relation $\Delta V^\circ \approx N_{\rm w} \bar{V}_{\rm w}$ for the MI–MII transition, where $\bar{V}_{\rm w}$ is the partial molar volume of water, for large PEG osmolytes between 1000 and 6000 Da an increase of 80 to 100 water molecules is calculated for the MI–MII transition. The change of the second virial coefficient ΔC is \sim 0.1 MPa $^{-2}$ and apparently corresponds to changes of \sim 0.01 MPa $^{-1}$ in osmotic compressibility.

Coming back to how the metarhodopsin equilibrium behaves in the presence of small PEGs (200-600 Da) as compared to large PEGs, the difference can be readily appreciated as follows. Initial addition of small PEG molecules shifts ln K linearly to the MII state up to a critical saturation point (Fig. 10). Medium-sized PEGs achieve this critical value at smaller concentrations and a lower maximum MII fraction versus the smallest- M_r PEGs. In the higher-concentration regime, above this critical value, the metarhodopsin equilibrium more closely resembles the large- $M_{\rm r}$ PEGs (Fig. 10). By fitting the osmotic pressure dependency curve as a piecewise function, we calculated thermodynamic values for the MI-MII transition, i.e., the change in hydration and the virial coefficient. At low concentration, small osmolytes initially penetrate the rhodopsin protein and stabilize the MII state through nonosmotic, chemical (quinary) interactions. As more osmolyte molecules crowd the binding region, they inhibit entry of further polymers as seen for large PEGs. Hence, osmotic effects become dominant beyond receptor saturation, where such a universal trend for small and large osmolytes (Figs. 9, 10) further supports our conclusion about increased hydration of rhodopsin upon light activation. The critical saturation point varies with the polymer size, because smaller osmolytes are more tightly packed within rhodopsin, and reach saturation at greater concentrations (Fig. 10).

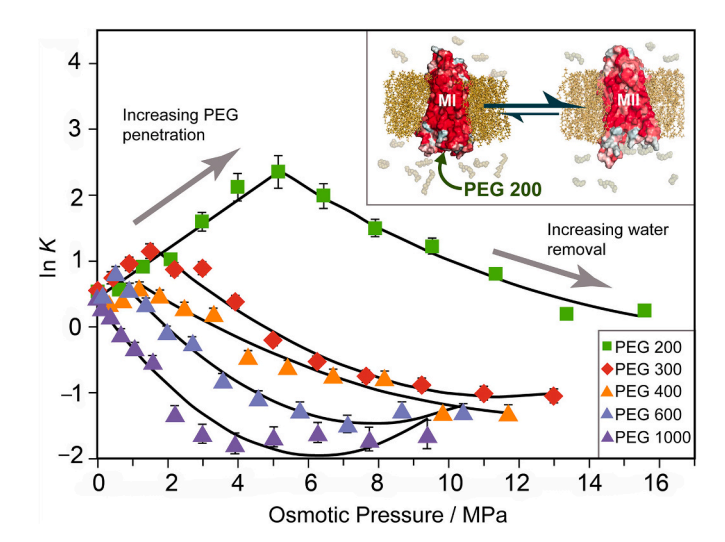


Fig. 10. Small polymer osmolytes stabilize active rhodopsin by replacing water until saturation is reached. Initially small osmolytes (PEG 200–PEG 600) forward shift ln *K* to the MII state. A saturation effect is observed beyond which the equilibrium is back shifted to MI, resembling dehydration by large osmolytes. As PEG size increases, the trend behaves more like the universal colligative behavior. Inset: small osmolytes such as PEG 200 penetrate the transducin binding cavity and stabilize the open active MII state until the cavity is saturated with small PEGs. Adapted from ref. [43]. Copyright (2022) National Academy of Sciences.

Our results show that the measured thermodynamic parameters of the MI-MII transition also correspond to the expected property of osmolyte saturation. With smaller PEGs, a slightly lower hydration volume is found (Fig. 5), together with less of a change ΔC in virial coefficient. Due to the small PEG replacing protein-associated water molecules in the low-concentration regime, fewer waters are available to withdraw from the protein in the osmotic regime, needing greater osmotic pressures to generate similar volumetric reductions. Accordingly, we obtain a less negative first-order term in the osmotic regime, and lower apparent hydration volume for the MI-MII transition for the small PEGs versus excluded larger PEGs. Furthermore, the stabilizing effect of PEG penetration is observed in the lower virial coefficient change ΔC for small PEGs. These small osmolytes penetrate and stabilize the protein in the lower-concentration regime, thus decreasing the variability in properties such as volumetric compressibility for the highconcentration regime. More strongly interacting PEGs should experience fewer number fluctuations within rhodopsin compared to water, corresponding to smaller volume fluctuations of hydrated MII that may typically give rise to a lower hydration compressibility or virial coefficient C in the active MII state.

6. Osmotic stress and hydrostatic pressure yield shifting of the metarhodopsin equilibrium

One of the striking features of the visual photoreceptor is that both hydrostatic pressure and osmotic stress shift the metarhodopsin equilibrium toward the preactive MI state [62]. However, their mechanisms of action are different. Hydrostatic pressure yields a change in the molar volume of the protein (i.e., density), but not a change in the number of water molecules $N_{\rm w}$ in the receptor (a thermodynamically closed system). The increase in density may entail the penetration of water molecules into small cavities or voids of rhodopsin, void collapse, or alternatively, a higher-density solvation shell versus the bulk solvent [63]. In the case of osmotic pressure, there is a change in protein hydration across the (virtual) Gibbs dividing surface that separates the interior rhodopsin volume from the external bulk water (thermodynamically an open system). The two methods are complementary, and together they give a more precise view of rhodopsin activation in a hydrated lipid membrane. Analogously to the effect of pressure on protein folding [64], the preactive MI state under pressure can be viewed as more densely packed in which void volume and solvent in internal cavities are minimized. On the other hand, active MII is a less dense state with greater water content after photoactivation.

The question then arises: Why is the active MII state favored at higher concentrations of large molar mass osmolytes (where the effect of compressibility may occur), while hydrostatic pressure changes the equilibrium to the preactive MI state? Here we recall that the second virial coefficient in formula (4) can be challenging to interpret. For example, if the main contribution to the second term is osmotic compressibility, then the positive sign indicates that it increases upon transition to the active MII state, due to fluctuations in the hydration volume of the protein. The greater volumetric fluctuations are given by $\sigma_{\rm V}^2 = \bar{V}^2 - \bar{V}^2 = k_{\rm B} T \kappa \bar{V}$ where $\sigma_{\rm V}^2$ is the variance of the distribution for an (N,P,T) ensemble, in good agreement with the sponge model of a solvent-swollen protein [9]. Greater volumetric fluctuations of the hydrated MII state lead to entropic stabilization of the active receptor, offsetting the enthalpic penalty due to its formation [8,9,43,65,66]. These entropic increases are associated with the hydrated protein volume and are large compared to any entropic reduction from the solvent molecules themselves. The new water molecules of hydration in active MII still exist in a predominantly bulk-like state—as indicated by osmotic stress techniques which detect weakly bound water [67], and molecular dynamics (MD) simulations showing rapid exchange with the protein [10,39]. Such colligative properties are entropic in nature and stand in stark contrast to the tightly bound water molecules visualized

by X-ray crystal structures [5,49,68] and radiolytic protein footprinting [49].

Alternatively, the contribution to the second virial coefficient may be related to quinary interactions of osmolytes with the protein itself that have an enthalpic origin. The specific chemistry could shift the equilibrium to the active MII state by interactions with the Glu¹³⁴ hydration site mentioned above, as in the case of cationic lipids [69]. For large osmolytes at low concentrations, an equilibrium shift to the preactive MI state is favored. As the concentration of osmolytes increases, they can penetrate more into rhodopsin, and the quinary interactions with the protein can become greater. The compressibility changes and specific interactions of large osmolytes with the protein could both contribute to the difference of the second virial coefficient ΔC in the nonlinear term of formula (4). Another aspect is that both large osmolytes and hydrostatic pressure yield similar effects on rhodopsin activation, and they also have comparable influences on lipid bilayer properties (Fig. 6) [30,70]. Yet, for small osmolytes membrane dehydration shifts the equilibrium oppositely to the active MII state [47], while for large osmolytes the lipid influence is negligible versus the direct osmotic effect on the receptor, which favors the closed inactive conformation. Since the osmolyte effects on the protein are clearly distinguished and a universal colligative behavior is observed [43], we currently favor an interpretation in terms of volumetric changes and compressibility.

Our explanation for triggering of the light-induced changes is based on the hydrostatic and osmotic pressure dependence of the rhodopsin activation equilibrium [9,43]. Here we are inspired by the work of Hans Frauenfelder et al. [71,72] for the idea of a hierarchical energy landscape (EL), which we now extend to include the protein softness [73] based on pressure studies. The current research follows pioneering experiments with rhodopsin [48,74,75-78] and applies these insights to protein interactions with the lipids and aqueous solvent [14], as well as effector proteins [42]. In this aspect, rhodopsin might be called "the hydrogen atom of membrane biology" by analogy with myoglobin for globular proteins [79]. Indeed, many of the foundational concepts of membrane biophysics were first discovered with visual rhodopsin [74–76] leading to the textbook fluid-mosaic model [80]. Previously, the function of rhodopsin—namely, detection of a photon of visible light and its conversion into a nerve impulse—was considered to be straightforward, simple, and fully understood. But the situation is now changed, due to breakthroughs in understanding its functional interactions with the soft biomembrane matter (lipids and associated water). For example, allosterism of rhodopsin was previously thought to be confined to the protein and retinal cofactor—vet recent work shows that the protein interacts with the lipids and the aqueous solvent in the visual mechanism [14,43]. Far from the textbook view, rhodopsin gives a new paradigm that touches many aspects of biology, chemistry, and physics. It impacts our understanding of the soft membrane matter in transformative ways linked to current trends in structural biology and cellular signaling.

7. Energy landscape manifests basins of attraction for rhodopsin photoactivation

As an illustration, let us consider a two-tier energy landscape as introduced for both proteins [72,81] and lipids [82]. In both cases the dynamics are broadly separated into fast local motions and slower collective fluctuations [81,82]. For proteins, the local (β) fluctuations originate from the hydration shell and may involve interstitial solvation of cavities or voids (e.g., due to amino acid side chains, methyl groups, or peptide backbone motions). Alternatively, the collective (α) fluctuations arise from the larger-scale protein dynamics within its hydrated volume, which are coupled to the bulk solvent (e.g., helical displacements, hydrogen-bonded networks, and/or conserved switches). Each molecule is different and hence a thermodynamic average or statistical mechanical ensemble is applicable [83]. The high-dimensional land-scape with its hills and valleys can be flattened onto a 2-dimensional

plane that shows the hierarchy as the basins of attraction, e.g., corresponding to the various tiers or energy levels [72]. Experiments indicate that the β -fluctuations are coupled to the hydration shell and populate the β -basins, while conversely the α -fluctuations explore the α -basins through coupling to the bulk solvent. By studying the effects of both hydrostatic pressure and osmotic pressure, we can further examine how the energy landscape might suggest "slaving" of the fluctuations to the solvent driving force [72,79]. Analogously, for membrane lipids, the local dynamics of the acyl chains (e.g., trans–gauche isomerizations) are coupled to the hydrocarbon microviscosity (η), while the collective motions involve order-director fluctuations (ODF) that are related to the bilayer elasticity (κ) [84–86].

Experimentally the energy landscape can be probed by investigating the effects of temperature [72] as well as pressure [64,87] as the relevant thermodynamic variables of state. The force-based measurements involve either hydrostatic pressure [62,88] or osmotic pressure [23, 38 43] to study the protein dynamics. Just as time- and temperaturedependent studies explore the protein motions, effects of pressure can elucidate the volumetric shape fluctuations that control membrane protein functions. Relatively large values of the hydrostatic pressure (up to ~7000 atm) can force water molecules into the protein interior, e.g., into small cavities or voids [64,87], where the large energies manifest the strong interactions with water. As a result, hydrostatic pressure can uncover the local β -fluctuations that are strongly coupled to the solvent shell, giving the β -basins of the microscopic closed system. Conversely, the smaller osmotic pressures [23,43] can withdraw or force water from the hydrated protein volume into the surrounding solvent of the microscopic open system. Because the osmotic pressures are smaller, they act on the α -fluctuations that are coupled to the bulk solvent, as represented by the α -basins of the hierarchical energy landscape.

However, what is sometimes neglected is that the hydration volume may itself depend on pressure (either hydrostatic or osmotic). With the above thinking we can then separate the compressibility due to either the hydrostatic pressure [62,89,90] or osmotic pressure [43] into contributions from the β - and α -fluctuations, respectively, keeping ergodicity in mind [83]. The combined hydrostatic pressure and osmotic pressure studies explore the various levels of the EL due to protein interactions with water [42,43,87] and/or the membrane lipids [30,32], and introduce the hierarchical protein softness in conjunction with the α -compressibility and β -compressibility. Following Perera et al. [9], the local compressibility (κ) due to volumetric β -fluctuations and the compressibility due to collective α -fluctuations are considered separately. Studies of rhodopsin show the activation equilibrium after light absorption is shifted to the preactive MI state by large hydrostatic pressures (up to ~7000 atm) [62,89] and smaller osmotic pressures (up to \sim 100-150 atm) [42,43]. Both force-based measures drive the movements of water into or out of the protein [9], yet they act differently on the levels or tiers of the EL corresponding to the β - and α -basins of attraction. Relatively large hydrostatic pressures involve greater energies and act on the local β -fluctuations within the β -basins, while the osmotic pressures entail smaller energies and affect the collective α -fluctuations of the individual α -basins. For rhodopsin, we propose the hydrostatic pressure (P) forces water into the protein due to the strong local solvation as described by the β -compressibility. Alternatively, the osmotic pressure (stress) (Π) affects the collective domain motions due to the energetically weaker interactions with the bulk solvent as manifested by the α -compressibility. Combined pressure measurements give an experimental strategy for exploring the energy landscape in addition to temperature as a thermodynamic state variable [72].

We now come back to further explaining the backshifting of the metarhodopsin equilibrium by hydrostatic and osmotic pressure [42,62,89]. In the case of rhodopsin, we propose that the local volumetric β -compressibility is greater in the preactive MI state than the active MII state. Relatively large values of the hydrostatic pressure can selectively force water into the MI state giving a volumetric decrease, e. g., by disrupting hydrogen-bonded water networks of the solvent shell.

For the active MII state, however, the collective α -compressibility can be greater due to the less tightly bound bulk solvent. Because it is saturated with water, additional solvent cannot be forced into the protein as in the preactive MI state. The greater α -compressibility of the active MII state versus the preactive MI state may be due to collective tilting of the transmembrane helices observed with site-directed spin-labeling [18,77] and time-resolved X-ray solution scattering [12]. The changes in β - and α -compressibilities can evolve as the energy flows within the protein due to unlocking the active receptor state. Volumetric fluctuations of the active MII receptor may thus underlie the G-protein (transducin) binding and release in the visual mechanism [42].

Often it is stated that the effects of hydrostatic pressure and osmotic pressure on proteins or lipid membranes are different—but this is only partially true. In our view "pressure is pressure" (force per unit area) [9,30], and the distinction involves only the force and whether the system is closed or open [43]. For rhodopsin, we propose that the application of hydrostatic pressure drives the hydration water into the smaller protein cavities, while osmotic pressure forces water out of the larger protein pockets or clefts into the bulk solvent. Hydrostatic pressure acts on the protein plus solvent within the microscopic closed system, whereas osmotic pressure acts on the protein separated from the solvent by the semipermeable Gibbs dividing surface (virtual membrane) of the microscopic open system [30,32,43]. The greater β -compressibility of the preactive MI state allows water to be forced into the protein versus active MII, yielding an overall volumetric decrease under large hydrostatic pressures (up to ~7000 atm). Conversely, the osmotic force acts like an internal pressure within the hydrated protein volume. It drives water molecules into the surrounding solution to equilibrate the solvent chemical potential, e.g., due to hydrophilic polymers like polyethylene glycol (PEG). Notably osmotic pressure (stress) entails lower magnitude forces (up to ~150 atm) versus hydrostatic pressure because the coupling interactions with bulk water are weaker than for the solvent shell. In either case, backshifting of the metarhodopsin equilibrium occurs upon light activation under the applied external force. Although the back shifting is in the same direction, the total volume change is less for the local β -fluctuations (~3–6 water molecules) than for the larger collective α -fluctuations (~80–100 water molecules). The explanation is that molecular contacts and ionic locks in the active MII state are disrupted that allow the protein volumetric fluctuations to be coupled to the large influx (flood) of water described by our sponge model for rhodopsin activation [42].

8. Significance for structural biology: hydration-dehydration cycling of rhodopsin

For visual rhodopsin the proposed water movements are significant for its light signaling function—they open up new ways of thinking about its interactions with effector proteins like transducin. Following light absorption, the water influx into the rhodopsin interior allows proton uptake to occur via Glu¹³⁴ of the conserved E(D)RY motif, yielding the high-affinity MII_bH⁺ substate. Exposure of the G-protein recognition site enables Gt-GDP to bind via the α 5 helix of the transducin C-terminus (Fig. 11). Still, the rapid transducin activation rate ensures it cannot remain strongly bound, but rather the G-protein must be released quickly after GDP-GTP nucleotide exchange. Hydration-dehydration cycling involving rhodopsin transmembrane helical fluctuations satisfies the criteria of high G-protein binding and unbinding rates (Fig. 11) [42]. After transducin binding rhodopsin is able to dehydrate, shifting the equilibrium back to the preactive MI state. Exchange of GTP for GDP then leads to dissociation of the transducin $G_{\beta\gamma}$ subunits, locally withdrawing water analogous to large polymer osmolytes. Transducin is able to catalyze its own release by expelling the G_{α} -GTP subunit facilitating the next round of the G-protein activation cycle. Rhodopsin activation is coupled to large-scale changes in protein hydrated volume as shown by osmotic stress studies that provide clear evidence of an influx of ~80–100 water molecules into the protein going from the preactive MI

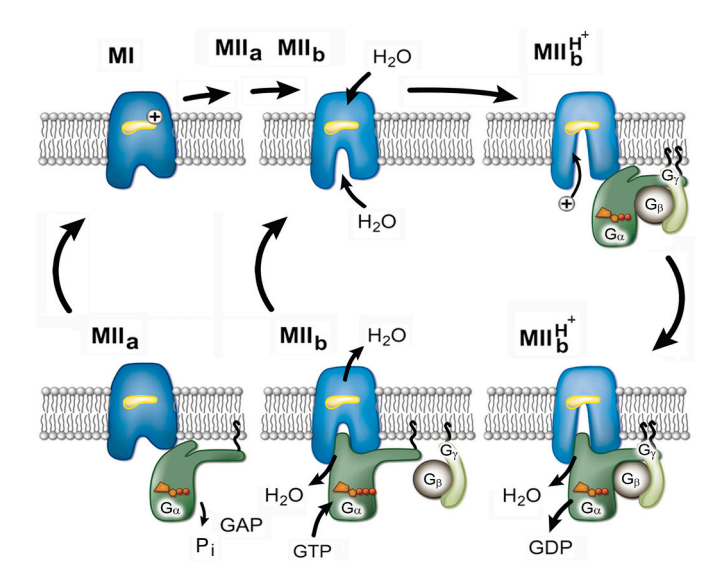


Fig. 11. Hydration-dehydration cycling explains catalytic activation of transducin by light-activated rhodopsin. Coupling of water influx and efflux by rhodopsin (blue) to binding and unbinding of the G-protein transducin (green) accounts for rapid visual signaling by a sponge-like allosteric mechanism. (Upper left) Rhodopsin enters cycle in the low-hydration low-affinity MI state by visible light isomerization of the retinal protonated Schiff base (SB) (yellow). (Upper middle) In the ${\rm MII_b}$ substate [16] the SB becomes deprotonated breaking the ionic lock to the Glu¹¹³/Glu¹⁸¹ complex counterion (first protonation switch). Transmembrane helix TM6 tilts away from the helical bundle [16] initiating influx of water into the transducin-binding cleft [10] (MII_b). (Upper right) Water influx into the protein facilitates proton uptake via Glu^{134} of the conserved E(D)RY motif giving the high-hydration high-affinity MII_bH⁺ substate (second protonation switch). (Lower right) Exposure of the Gprotein binding cleft allows binding of Gt·GDP via the α5 helix of the transducin C-terminus. (Lower middle) Exchange of GTP for GDP dissociates the transducin G_{fiv} subunits dehydrating rhodopsin and giving the partially hydrated MIIb substate. (Lower left) Transducin catalyzes its own release by pinching off the G_{α} ·GTP subunit, while the GTPase-activating protein (GAP) terminates signaling by GTP hydrolysis on transducin. Adapted from ref. [42]. Reproduced by permission of Wiley-VCH Verlag GmbH & Co. KGaA Weinheim.

to the active MII state. The opposing effects of polymer osmolytes on the metarhodopsin equilibrium uncover how large molar mass solutes are excluded from rhodopsin. They dehydrate the active state of the receptor according to Le Châtelier's principle, while small osmolytes penetrate the protein increasing the active state fraction. Hydration also affects the interaction of the receptor with peptide analogues of its cognate G-protein whose binding affinity may change in accord with a hydration-mediated sponge model. In the new paradigm, water acts as an allosteric modulator of rhodopsin interactions with effector proteins such as transducin. Whether functional water movements as studied by pressure-based techniques occur in other GPCRs, and whether disease-causing mutations involve changes in water influx, pose interesting future questions for drug discovery.

Author statement

During the preparation of this work, the authors did not use AI and AI-related software. All contents were written by the authors. All authors have seen and approved the submitted version of this manuscript.

Declaration of Competing Interest

The authors declare that they have no known competing financial interests or personal relationships that could have appeared to influence the work reported in this paper.

Acknowledgments

We dedicate this paper to Professor Richard M. Epand in recognition of his many sustained contributions to biophysics throughout his entire career. M.F.B. is particularly grateful to Richard Epand for many engaging discussions and conversations, and with appreciation of his warm collegiality. A.V.S. acknowledges partial support from Saint-Petersburg State University (grant 104236506). This work was sponsored by the U.S. National Science Foundation (CHE 1904125 and MCB 1817862) and by the U.S. National Institutes of Health (EY012049 and EY026041) (to M.F.B.).

References

- N.R. Latorraca, A.J. Venkatakrishnan, R.O. Dror, GPCR dynamics: structures in motion, Chem. Rev. 117 (2017) 139–155.
- [2] D. Hilger, M. Masureel, B.K. Kobilka, Structure and dynamics of GPCR signaling complexes, Nat. Struct. Mol. Biol. 25 (2018) 4–12.
- [3] W.I. Weis, B.K. Kobilka, The molecular basis of G protein-coupled receptor activation, Annu. Rev. Biochem. 89 (2018) 897–919.
- [4] A.J. Venkatakrishnan, A.K. Ma, R. Fonseca, N.R. Latorraca, B. Kelly, R.M. Betz, C. Asawa, B.K. Kobilka, R.O. Dror, Diverse GPCRs exhibit conserved water networks for stabilization and activation, Proc. Natl. Acad. Sci. U. S. A. 116 (2019) 3288–3293
- [5] H.-W. Choe, Y.J. Kim, J.H. Park, T. Morizumi, E.F. Pai, N. Krauβ, K.P. Hofmann, P. Scheerer, O.P. Ernst, Crystal structure of metarhodopsin II, Nature 471 (2011) 651–655.
- [6] S.G.F. Rasmussen, H.-J. Choi, J.J. Fung, E. Pardon, P. Casarosa, P.S. Chae, B. T. DeVree, D.M. Rosenbaum, F.S. Thian, T.S. Kobilka, A. Schnapp, I. Konetzki, R. K. Sunahara, S.H. Gellman, A. Pautsch, J. Steyaert, W.I. Weis, B.K. Kobilka, Structure of a nanobody-stabilized active state of the β_2 adrenoceptor, Nature 469 (2011) 175–189.
- [7] Y. Kang, X.E. Zhou, X. Gao, Y. He, W. Liu, A. Ishchenko, A. Barty, T.A. White, O. Yefanov, G.W. Han, Q. Xu, P.W. de Waal, J. Ke, M.H.E. Tan, C. Ghai Zhang, A. Arne Moeller, G.M. West, B.D. Pascal, N. Van Eps, L.N. Caro, S.A. Vishnivetskiy, R. J. Lee, K.M. Suino-Powell, X. Gu, K. Pal, J. Ma, X. Zhi, S. Boutet, G.J. Williams, M. Messerschmidt, C. Gati, N.A. Zatsepin, D. Wang, D. James, S. Basu, S. Roy-Chowdhury, C.E. Conrad, J. Coe, H. Liu, S. Lisova, C. Kupitz, I. Grotjohann, R. Fromme, Y. Jiang, M. Tan, H. Yang, J. Li, M. Wang, Z. Zheng, D. Li, N. Howe, Y. Zhao, J. Standfuss, K. Diederichs, Y. Dong, C.S. Potter, B. Carragher, M. Caffrey, H. Jiang, H.N. Chapman, J.C.H. Spence, P. Fromme, U. Weierstall, O.P. Ernst, V. Katritch, V. Gurevich, P.R. Griffin, W.L. Hubbell, R.C. Stevens, V. Cherezov, K. Melcher, H.E. Xu, Crystal structure of rhodopsin bound to arrestin by femtosecond X-ray laser, Nature 523 (2015) 561–567.
- [8] U.R. Shrestha, S.M.D.C. Perera, D. Bhowmik, U. Chawla, E. Mamontov, M. F. Brown, X.-Q. Chu, Quasi-elastic neutron scattering reveals ligand-induced protein dynamics of a G-protein-coupled receptor, J. Phys. Chem. Lett. 7 (2016) 4130–4136
- [9] S.M.D.C. Perera, U. Chawla, U.R. Shrestha, D. Bhowmik, A.V. Struts, S. Qian, X.-Q. Chu, M.F. Brown, Small-angle neutron scattering reveals energy landscape for rhodopsin photoactivation, J. Phys. Chem. Lett. 9 (2018) 7064–7071.
- [10] N. Leioatts, B.M. Mertz, K. Martínez-Mayorga, T.D. Romo, M.C. Pitman, S.E. Feller, A. Grossfield, M.F. Brown, Retinal ligand mobility explains internal hydration and reconciles active rhodopsin structures, Biochemistry 53 (2014) 376–385.
- [11] L.A. Salas-Estrada, N. Leioatts, T.D. Romo, A. Grossfield, Lipids alter rhodopsin function via ligand-like and solvent-like interactions, Biophys. J. 114 (2018) 255 267
- [12] E. Malmerberg, P.H.M. Bovee-Geurts, G. Katona, X. Deupi, D. Arnlund, C. Wickstrand, L.C. Johansson, S. Westenhoff, E. Nazarenko, G.F.X. Schertler, A. Menzel, W.J. de Grip, R. Neutze, Conformational activation of visual rhodopsin in native disc membranes, Sci. Signal. 8 (2015), ra26.
- [13] M.F. Brown, Curvature forces in membrane lipid-protein interactions, Biochemistry 51 (2012) 9782–9795.
- [14] M.F. Brown, Soft matter in lipid-protein interactions, Annu. Rev. Biophys. 46 (2017) 379–410.
- [15] E. Zaitseva, M.F. Brown, R. Vogel, Sequential rearrangement of interhelical networks upon rhodopsin activation in membranes: the Meta II_a conformational substate, J. Am. Chem. Soc. 132 (2010) 4815–4821.
- [16] B. Knierim, K.P. Hofmann, O.P. Ernst, W.L. Hubbell, Sequence of late molecular events in the activation of rhodopsin, Proc. Natl. Acad. Sci. U. S. A. 104 (2007) 20290–20295.
- [17] M. Mahalingam, K. Martínez-Mayorga, M.F. Brown, R. Vogel, Two protonation switches control rhodopsin activation in membranes, Proc. Natl. Acad. Sci. U. S. A. 105 (2008) 17795–17800.
- [18] C. Altenbach, A.K. Kusnetzow, O.P. Ernst, K.P. Hofmann, W.L. Hubbell, Highresolution distance mapping in rhodopsin reveals the pattern of helix movement due to activation. Proc. Natl. Acad. Sci. U. S. A. 105 (2008) 7439–7444.
- [19] O. Soubias, K. Gawrisch, The role of the lipid matrix for structure and function of the GPCR rhodopsin, Biochim. Biophys. Acta 1818 (2012) 234–240.
- [20] S.D.E. Fried, J.W. Lewis, I. Szundi, K. Martinez-Mayorga, M. Mahalingam, R. Vogel, D.S. Kliger, M.F. Brown, Membrane curvature revisited — the archetype of

- rhodopsin studied by time-resolved electronic spectroscopy, Biophys. J. 120 (2021) 440–452.
- [21] Z. Salamon, Y. Wang, M.F. Brown, H.A. Macleod, G. Tollin, Conformational changes in rhodopsin probed by surface plasmon resonance spectroscopy, Biochemistry 33 (1994) 13706–13711.
- [22] Z. Salamon, M.F. Brown, G. Tollin, Plasmon resonance spectroscopy: probing molecular interactions within membranes, Trends Biochem. Sci. 24 (1999) 213–219.
- [23] M.F. Colombo, D.C. Rau, V.A. Parsegian, Protein solvation in allosteric regulation: a water effect on hemoglobin, Science 256 (1992) 655–659.
- [24] C. Reid, R.P. Rand, Probing protein hydration and conformational states in solution, Biophys. J. 72 (1997) 1022–1030.
- [25] G.D. Dzingeleski, R. Wolfenden, Hypersensitivity of an enzyme reaction to solvent water, Biochemistry 32 (1993) 9143–9147.
- [26] J. Zimmerberg, F. Benzanilla, V.A. Parsegian, Solute inaccessible aqueous volume changes during opening of the potassium channel of the squid giant axon, Biophys. J. 57 (1990) 1049–1064.
- [27] I. Vodanoy, S.M. Bezrukov, V.A. Parsegian, Probing alamethicin channels with water-soluble polymers. Size-modulated osmotic action, Biophys. J. 65 (1993) 2097–2105
- [28] M.D. Rayner, J.G. Starkus, P.C. Ruben, D.A. Alicata, Voltage-sensitive and solvent-sensitive processes in ion channel gating. Kinetic effects of hyperosmolar media on activation and deactivation of sodium channels, Biophys. J. 61 (1992) 96–108.
- [29] J.A. Kornblatt, G. Hui Bon Hoa, A nontraditional role for water in the cytochrome c oxidase reaction, Biochemistry 29 (1990) 9370–9376.
- [30] K.J. Mallikarjunaiah, A. Leftin, J.J. Kinnun, M.J. Justice, A.L. Rogozea, H. I. Petrache, M.F. Brown, Solid-state ²H NMR shows equivalence of dehydration and osmotic pressures in lipid membrane deformation, Biophys. J. 100 (2011) 98–107.
- [31] J.J. Kinnun, K.J. Mallikarjunaiah, H.I. Petrache, M.F. Brown, Elastic deformation and area per lipid of membranes: atomistic view from solid-state deuterium NMR spectroscopy, Biochim. Biophys. Acta 1848 (2015) 246–259.
- [32] K.J. Mallikarjunaiah, J.J. Kinnun, H.I. Petrache, M.F. Brown, Flexible lipid nanomaterials studied by NMR spectroscopy, Phys. Chem. Chem. Phys. 21 (2019) 18422–18457.
- [33] J.Y.A. Lehtonen, K.J. Kinnunen, Changes in the lipid dynamics of liposomal membranes induced by poly(ethylene glycol): free volume alterations revealed by inter- and intramolecular excimer-forming phospholipid analogs, Biophys. J. 66 (1994) 1981–1990.
- [34] T.R. Molugu, S. Lee, M.F. Brown, Concepts and methods of solid-state NMR spectroscopy applied to biomembranes, Chem. Rev. 117 (2017) 12087–12132.
- [35] J.T. McCown, E. Evans, S. Diehl, H.C. Wiles, Degree of hydration and lateral diffusion in phospholipid multibilayers, Biochemistry 20 (1981) 3134–3138.
- [36] D.C. Mitchell, B.J. Litman, Effect of protein hydration on receptor conformation: decreased levels of bound water promote metarhodopsin II formation, Biochemistry 38 (1999) 7617–7623.
- [37] M. Straume, D.C. Mitchell, J.L. Miller, B.J. Litman, Interconversion of metarhodopsins I and II: a branched photointermediate decay model, Biochemistry 29 (1990) 9135–9142.
- [38] V.A. Parsegian, R.P. Rand, D.C. Rau, Macromolecules and water: probing with osmotic stress, Methods Enzymol. 259 (1995) 43–94.
- [39] A. Grossfield, M.C. Pitman, S.E. Feller, O. Soubias, K. Gawrisch, Internal hydration increases during activation of the G-protein-coupled receptor rhodopsin, J. Mol. Biol. 381 (2008) 478–486.
- [40] J. Feng, M.F. Brown, B. Mertz, Retinal flip in rhodopsin activation? Biophys. J. 108 (2015) 2767–2770.
- [41] A.V. Botelho, T. Huber, T.P. Sakmar, M.F. Brown, Curvature and hydrophobic forces drive oligomerization and modulate activity of rhodopsin in membranes, Biophys. J. 91 (2006) 4464–4477.
- [42] U. Chawla, S.M.D.C. Perera, S.D.E. Fried, A.R. Eitel, B. Mertz, N. Weerasinghe, M. C. Pitman, A.V. Struts, M.F. Brown, Activation of the G-protein-coupled receptor rhodopsin by water, Angew. Chem. Int. Ed. 60 (2021) 2288–2295.
- [43] S.D.E. Fried, K.S.K. Hewage, A.R. Eitel, A.V. Struts, N. Weerasinghe, S.M.D. C. Perera, M.F. Brown, Hydration-mediated G-protein-coupled receptor activation, Proc. Natl. Acad. Sci. U. S. A. 119 (2022), e2117349119.
- [44] J.F. Nagle, S. Tristram-Nagle, Structure of lipid bilayers, Biochim. Biophys. Acta 1469 (2000) 159–195.
- [45] J.F. Nagle, D.A. Wilkinson, Lecithin bilayers. Density measurements and molecular interactions, Biophys. J. 23 (1978) 159–175.
- [46] Y. Wang, A.V. Botelho, G.V. Martinez, M.F. Brown, Electrostatic properties of membrane lipids coupled to metarhodopsin II formation in visual transduction, J. Am. Chem. Soc. 124 (2002) 7690–7701.
- [47] C.J. López, M.R. Fleissner, Z. Guo, A.K. Kusnetzow, W.L. Hubbell, Osmolyte perturbation reveals conformational equilibria in spin-labeled proteins, Protein Sci. 18 (2009) 1637–1652.
- [48] K. Palczewski, T. Kumasaka, T. Hori, C.A. Behnke, H. Motoshima, B.A. Fox, I. Le Trong, D.C. Teller, T. Okada, R.E. Stenkamp, M. Yamamoto, M. Miyano, Crystal structure of rhodopsin: a G protein-coupled receptor, Science 289 (2000) 739–745.
- [49] T.E. Angel, S. Gupta, B. Jastrzebska, K. Palczewski, M.R. Chance, Structural waters define a functional channel mediating activation of the GPCR, rhodopsin, Proc. Natl. Acad. Sci. U. S. A. 106 (2009) 14367–14372.
- [50] A. Sandoval, S. Eichler, S. Madathil, P.J. Reeves, K. Fahmy, R.A. Böckmann, The molecular switching mechanism at the conserved D(E)RY motif in class-A GPCRs, Biophys. J. 111 (2016) 79–89.
- [51] I.A. Shkel, D.B. Knowles, M.T. Record Jr., Separating chemical and excluded volume interactions of polyethylene glycols with native proteins: comparison with PEG effects on DNA helix formation, Biopolymers 103 (2015) 517–527.

- [52] K. Matsuzaki, K. Sugishita, N. Ishibe, M. Ueha, S. Nakata, K. Miyajima, R.M. Epand, Relationship of membrane curvature to the formation of pores by magainin 2, Biochemistry 37 (1998) 11856–11863.
- [53] R.M. Epand, H.J. Vogel, Diversity of antimicrobial peptides and their mechanisms of action, Biochim. Biophys. Acta 1462 (1999) 11–28.
- [54] R.M. Epand, R.F. Epand, Lipid domains in bacterial membranes and the action of antimicrobial agents, Biochim. Biophys. Acta 1788 (2009) 289–294.
- [55] R.M. Epand, C. Walker, R.F. Epand, N.A. Magarvey, Molecular mechanisms of membrane targeting antibiotics, Biochim. Biophys. Acta 1656 (2016) 980–987.
- [56] R. Herrmann, M. Heck, P. Henklein, P. Henklein, C. Kleuss, K.P. Hofmann, O. P. Ernst, Sequence of interactions in receptor-G protein coupling, J. Biol. Chem. 279 (2004) 24283–24290.
- [57] R. Herrmann, M. Heck, P. Henklein, K.P. Hofmann, O.P. Ernst, Signal transfer from GPCRs to G proteins. Role of the $G\alpha$ N-terminal region in rhodopsin-transducin coupling, J. Biol. Chem. 281 (2006) 30234–30241.
- [58] R. Herrmann, M. Heck, P. Henklein, C. Kleuss, V. Wray, K.P. Hofmann, O.P. Ernst, Rhodopsin-transducin coupling: role of the Gα C-terminus in nucleotide exchange catalysis, Vis. Res. 46 (2006) 4582–4593.
- [59] U. Chawla, S.M.D.C. Perera, A.V. Struts, M.C. Pitman, M.F. Brown, Hydration mediated G-protein-coupled receptor activation, Biophys. J. 110 (2016) 83a.
- [60] C. Knight, G.A. Voth, The curious case of the hydrated proton, Acc. Chem. Res. 45 (2012) 101–109.
- [61] R. Vogel, S. Lüdeke, F. Siebert, T.P. Sakmar, A. Hirshfeld, M. Sheves, Agonists and partial agonists of rhodopsin: retinal polyene methylation affects receptor activation, Biochemistry 45 (2006) 1640–1652.
- [62] A.A. Lamola, T. Yamane, A. Zipp, Effects of detergents and high pressures upon the metarhodopsin I – metarhodopsin II equilibrium, Biochemistry 13 (1974) 738–745.
- [63] D.R. Martin, D.V. Matyushov, Dipolar nanodomains in protein hydration shells, J. Phys. Chem. Lett. 6 (2015) 407–412.
- [64] C.A. Royer, Revisiting volume changes in pressure-induced protein unfolding, Biochim. Biophys. Acta 1595 (2002) 201–209.
- [65] R.G. Matthews, R. Hubbard, P.K. Brown, G. Wald, Tautomeric forms of metarhodopsin, J. Gen. Physiol. 47 (1963) 215–240.
- [66] K.P. Hofmann, T.D. Lamb, Rhodopsin, light-sensor of vision, Prog. Retin. Eye Res. 93 (2023) 101116.
- [67] D.M. LeNeveu, P.R. Rand, V.A. Parsegian, Measurement of forces between lecithin bilayers, Nature 259 (1976) 601–603.
- [68] T. Okada, M. Sugihara, A.-N. Bondar, M. Elstner, P. Entel, V. Buss, The retinal conformation and its environment in rhodopsin in light of a new 2.2 Å crystal structure. J. Mol. Biol. 342 (2004) 571–583.
- [69] U. Chawla, Y. Jiang, W. Zheng, L. Kuang, S.M.D.C. Perera, M.C. Pitman, M. F. Brown, H. Liang, A usual G-protein-coupled receptor in unusual membranes, Angew. Chem. Int. Ed. 128 (2016) 588–592.
- [70] A. Brown, I. Skanes, M.R. Morrow, Pressure-induced ordering in mixed-lipid bilayers, Phys. Rev. E 69 (2004), 011913.
- [71] H. Frauenfelder, S.G. Sligar, P.G. Wolynes, The energy landscapes and motions of proteins, Science 254 (1991) 1598–1603.
- [72] H. Frauenfelder, G. Chen, J. Berendzen, P.W. Fenimore, H. Jansson, B. H. McMahon, I.R. Stroe, J. Swenson, R.D. Young, A unified model of protein dynamics, Proc. Natl. Acad. Sci. U. S. A. 106 (2009) 5129–5134.
- [73] G. Zaccai, How soft is a protein? A protein dynamics force constant measured by neutron scattering, Science 288 (2000) 1604–1607.
- [74] R.A. Cone, Rotational diffusion of rhodopsin in the visual receptor membrane, Nat. New Biol. 236 (1972) 39–43.
- [75] P.A. Liebman, G. Entine, Lateral diffusion of visual pigment in photoreceptor disk membranes, Science 185 (1974) 457–459.
- [76] M. Poo, R.A. Cone, Lateral diffusion of rhodopsin in the photoreceptor membrane, Nature 247 (1974) 438–441.
- [77] D.L. Farrens, C. Altenbach, K. Yang, W.L. Hubbell, H.G. Khorana, Requirement of rigid-body motion of transmembrane helices for light activation of rhodopsin, Science 274 (1996) 768–770.
- [78] J. Li, P.C. Edwards, M. Burghammer, C. Villa, G.F.X. Schertler, Structure of bovine rhodopsin in a trigonal crystal form, J. Mol. Biol. 343 (2004) 1409–1438.
- [79] H. Frauenfelder, B.H. McMahon, P.W. Fenimore, Myoglobin: the hydrogen atom of biology and a paradigm of complexity, Proc. Natl. Acad. Sci. U. S. A. 100 (2003) 8615–8617.
- [80] S.J. Singer, G.L. Nicolson, The fluid mosaic model of the structure of cell membranes, Science 175 (1972) 720–731.
- [81] P.W. Fenimore, H. Frauenfelder, B.H. McMahon, R.D. Young, Bulk-solvent and hydration-shell fluctuations, similar to α- and β-fluctuations in glasses, control protein motions and functions, Proc. Natl. Acad. Sci. U. S. A. 101 (2004) 14408–14413.
- [82] M.F. Brown, A.A. Ribeiro, G.D. Williams, New view of lipid bilayer dynamics from ²H and ¹³C NMR relaxation time measurements, Proc. Natl. Acad. Sci. U. S. A. 80 (1983) 4325–4329.
- [83] T. Hill, Introduction to Statistical Thermodynamics, Addison-Wesley, Reading, 1960.
- [84] M.F. Brown, Theory of spin-lattice relaxation in lipid bilayers and biological membranes. ²H and ¹⁴N quadrupolar relaxation, J. Chem. Phys. 77 (1982) 1576–1599.
- [85] S. Chakraborty, M. Doktorova, T.R. Molugu, R. Ashkar, How cholesterol stiffens unsaturated lipid membranes, Proc. Natl. Acad. Sci. U. S. A. 117 (2020) 21896–21905.
- [86] M. Doktorova, G. Khelashvili, R. Ashkar, M.F. Brown, Molecular simulations and NMR reveal how lipid fluctuations affect membrane mechanics, Biophys. J. 122 (2023) 984–1002.

- [87] G. Hummer, S. Garde, A.E. García, M.E. Paulaitis, L.R. Pratt, The pressure dependence of hydrophobic interactions is consistent with the observed pressure denaturation of proteins, Proc. Natl. Acad. Sci. U. S. A. 95 (1998) 1552–1555.
- [88] A. Zipp, W. Kauzmann, Pressure denaturation of metmyoglobin, Biochemistry 12 (1973) 4217–4228.
- [89] P.V. Attwood, H. Gutfreund, The application of pressure relaxation to the study of the equilibrium between metarhodopsin I and II from bovine retinas, FEBS Lett. 119 (1980) 323–326.
- [90] P.J. King, H. Gutfreund, Kinetic studies on the formation and decay of metarhodopsins from bovine retinas, Vis. Res. 24 (1984) 1471–1475.